Effects of Lip Thickness and Recess Length on Spray Characteristics in Gas Centered Double Swirl Injector for 400N Methane Rocket Engine

400N 메탄 로켓 엔진용 기체 중심 이중 스월 분사기에서 립 두께와 리세스 길이가 분무 특성에 미치는 영향

2019 년 2 월

서울대학교 대학원

기계항공공학부

이 예 승

Abstract

Effects of Lip Thickness and Recess Length on Spray Characteristics in Gas Centered Double Swirl Injector for 400N Methane Rocket Engine

Yeseung Lee

School of Mechanical and Aerospace Engineering

The Graduate School

Seoul National University

    The 400N class small rocket engine is widely used for applications such as apogee engine for geosynchronous satellite or attitude control engine for manned or unmanned spacecraft. Conventional small rocket engines have mostly used toxic and corrosive hypergolic propellants. In recent years, however, the development of reusable launch vehicles and manned space exploration projects have led to the development of small methane rocket engine in countries such as the United States, Russia, and China.

Methane is a hydrocarbon but a cryogenic liquid, and oxygen / methane propellant is a non-hypergolic propellant that requires an igniter. Therefore, the properties of methane are different from any other propellants for small rocket engine that is currently in use or developed. Also, since the methane engine has a short history of development and there are few cases of actual use, it seems that proper method of propellant mixing and injector type have not been established.

In this study, concept design of combustion chamber and injection system of small rocket engine with a single bipropellant injector was performed. Oxygen and methane are used as a propellant in this engine. After designing the geometry of the combustion chamber, the combustion patterns by the injection and mixing system according to the combination of the swirl and jet injectors were compared. The finite element analysis method was used for the comparison, and the type of the injector suitable for the engine was selected as the gas centered double swirl injector. This type of the injector was designed by calculating the individual geometry and performance of the liquid and the gas injector, and then coaxially arranging them.

The spray characteristics of the coaxial injector according to the variation of the lip thickness of the gas injector and the recess length were investigated by cold test. In the case of the external mixing without the recess length, the droplet size

decreased and the fluctuation of mass distribution was weakened as the lip thickness increased. When the recess length corresponds to the critical mixing, a flow of fine droplet like mist was observed inside the spray cone, which increased with decreasing lip thickness. When the recess length corresponds to the internal mixing, the atomization performance of the injector was lower than that of the critical mixing as a whole.

Contents

List of Tables

List of Figures

Nomenclature

F_c	Area of injector nozzle, m²
F_{ch}	Area of combustion chamber, m²
$\overline{F_{ch}}$	Contraction ratio
F_{cr}	Area of nozzle throat, m²
F_{in}	Area of tangential inlet, m²
k	Isentropic exponent
K_m	Mixing ratio
$\dot{m}$	Mass flow rate, kg/sec
$\dot{m}_{in,out}$	Mass flow at the inlet of the outer injector, kg/sec
$\dot{m}_\Phi$	Mass flow rate of the injector, kg/sec
p_{Ch}	Chamber pressure, Pa
p_{in}	Pressure at the inlet of the injector, Pa
p_{out}	Pressure at the outlet of the injector, Pa
$r_{c,out}$	Radius of the nozzle of the outer injector, m
T_{in}	Temperature at the inlet of the injector, K
W_{ox}	Velocity of oxidizer, m/s

W_{fu}	Velocity of fuel, m/s
β	Flow Coefficient, m/s
$\Delta P_{in,out}$	Pressure at the inlet of the outer injector, Pa
ρ_{out}	Density of the fluid of the outer injector, kg/m^3
μ	Viscosity, Pa $\cdot$ s
μ_{out}	Viscosity of the fluid of the outer injector, Pa $\cdot$ s

Chapter 1. INTRODUCTION

1.1 Background

A small rocket engine generally refers to an engine with a thrust of 0.01N to 1600N [1], and is used for orbital transition and attitude control in space. Among them, 400N class rocket engines are used in various ways such as apogee engine (TR-308, S400), reaction control system (R-4D), and main engine for planetary explorer (S400). Due to this versatility of operation, many types of 400N class engines have been developed and are in operation.

Small rocket engines have a short residence time of propellant because combustion of propellant takes place in a small volume. In addition, as shown in Figure 1.1, if the flame is formed too close to the injector head, the head will be damaged, and if it is formed too far away, the propellant will not completely burn. These design challenges must be solved in the development process, and it is important to achieve high atomization, mixing and combustion efficiency while avoiding thermal damage.

The injector is one of the major components affecting the combustion process of the rocket engine by participating in the atomization, evaporation and mixing of the

propellant [2] and determines the performance of the rocket engine together with the parameters such as the shape of the combustion chamber and the characteristics of propellant. In the case of small rocket engine, the cross-sectional area of the injector head is as small as a few centimeters, and the number of injecting elements is small. Therefore, it is difficult for the flame to uniformly form, and the liquid propellant may reach the combustion chamber wall. For this reason, the propellant fed by each injector will affect both the performance and the cooling of the engine, and proper injector design is essential in the development of small rocket engine.
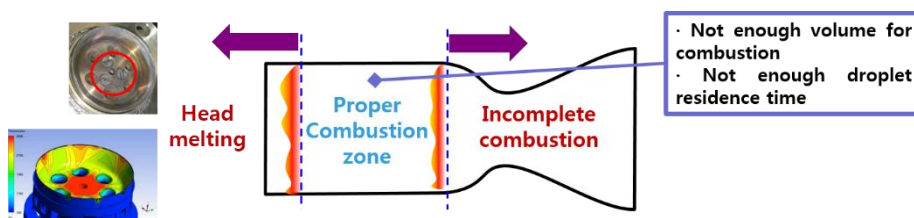
Figure 1.1 Characteristics of small rocket engine

Conventional small rocket engines mainly use hypergolic propellants (NTO + MMH, UDMH) which are highly corrosive and carcinogenic. These propellants are very dangerous to the human body, so special attention is required. In the United States, Russia and China, however, engine development is underway to replace toxic propellants with oxygen / methane.

According to the article [3], methane is not harmful enough to be supplied to the

home, and the pollution caused by incomplete combustion products is small. In addition, the cocking limit is high, so there is less soot after combustion. Moreover, methane has high efficiency, and it is used in a variety of industries, making it inexpensive and easy to supply.

Therefore, it is expected that small engines using methane will continue to be developed. However, it seems that the phase of the propellant, the suitable type of injector, and the cooling method of small methane engine have not been established because the development history of small methane engine is short. In addition, the selection range of them is wide due to the nature of methane having medium characteristics of hydrogen and kerosene. Therefore, further study is needed to find suitable components for small methane engines.

1.2 Overview of previous works

Engine Name	R-4D	TR-308	S400	11D458	17D16	Aerojet 445N	TR-408
Country	USA	USA	Europe	Russia	Russia	USA	USA
Manufacturer	Aerojet	Northrop Grumman	Astrium	NIIMASh	NIIMASh	Aerojet	Northrop Grumman
Propellants	NTO(MON-3) /MMH	N2O4/ N2H4	N2O4, MON-1 MON-3 /MMH	NTO/ UDMH	GOx/ Kerosene	LOX/ LCH4	GOX/ GCH4
Thrust [N]	489	470	418.3	392.4	196.2	445	445
Chamber Pressure [bar]	6.84	-	10	-	-	12	-
Injector Type	Doublet Impinging	Pintle	Double Swirl x 1	Double Swirl x 1 + Jet(cooling)	Jet + Jet (Internal mixing)	Triplet Impinging	Pintle
Usage	Apollo RCS	Apogee Engine	Apogee & Exploration	ISS RCS	Buran RCS	RCS & Exploration	RCS & Exploration

Table 1.1 Examples of small rocket engines [4-13]

Conventional engines have mainly used hypergolic propellants because of operational advantages. These engines include the US R-4D, TR-308, European S400, and the Russian 11D458. The R-4D was used for the Apollo spacecraft [4], the TR-308 and S400 were mainly used for satellites [5,6], and the 11D458 were used for RCS of the Mir and ISS [8].

The injectors of these engines can be divided into impinging type, pintle type, and double swirl type. In particular, the engines with double swirl injector such as the European Airbus Astrium S400 engine and the Russian NIIMash's 11D458 are mainly composed of a single bipropellant injector [7,9].
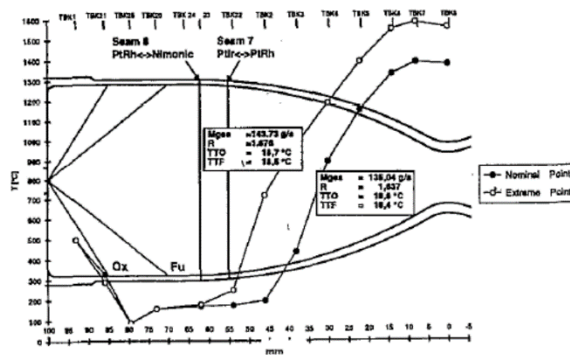
Figure 1.2 Schematic of Astrium S400 engine [7]
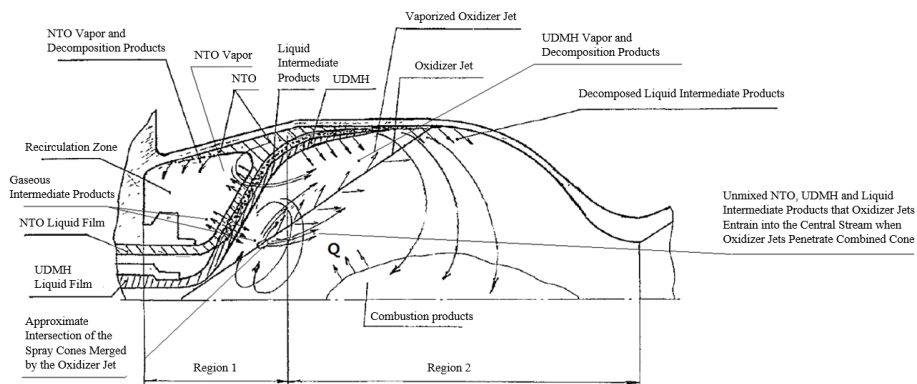
Figure 1.3 Schematic of NIIMASh 11D458 engine [9]

According to the literature [7,9], the two engines mentioned above use hydrazine type (MMH, UDMH) fuel and nitric oxide type oxidizer. In both cases, the oxidizer is located outside of the injector, and the spray angle of the oxidizer is larger than the fuel. This arrangement causes the oxidizer to have a cooling effect on the wall.

Moreover, depending on the material of the combustion chamber, and the

relationship between the distribution of the combustion products, and the shape of the combustion chamber, it may be necessary to apply an additional cooling system. For example, the Russian engine shown in Figure 1.3, a jet injector mounted inside the coaxial injector forms an additional oxidizer cooling film at the rear of the combustion chamber [9]
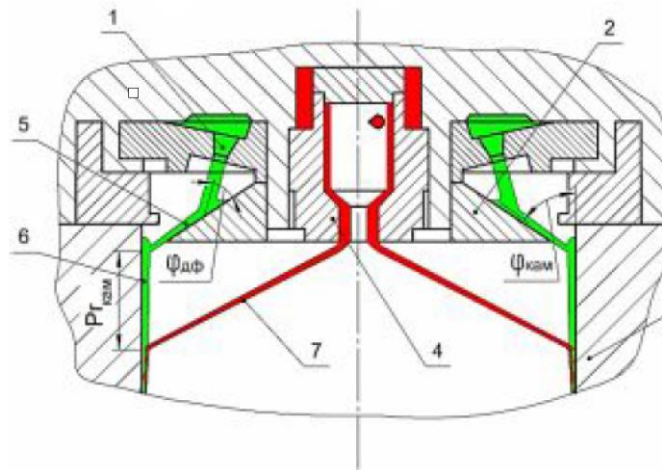
Figure 1.4 Schematic of KBKhM S5.165 engine [14]

There are also various types of small engines using swirl injectors, one of which is shown in Figure 1.4. According to the article [14], in the combustion chamber of the engine, fuel is injected at the central swirl injector and the jet injector injects the oxidizer to the deflector annularly surrounding the combustion chamber. The injected oxidizer impinges on the deflector and then flows along the wall, forming an oxidizer film. This film collides with the fuel cone injected from the swirl injector

6

and burns.

In recent years, a small engine using methane which is harmless to the human body has been developed for the purpose of utilization in manned space exploration [13].
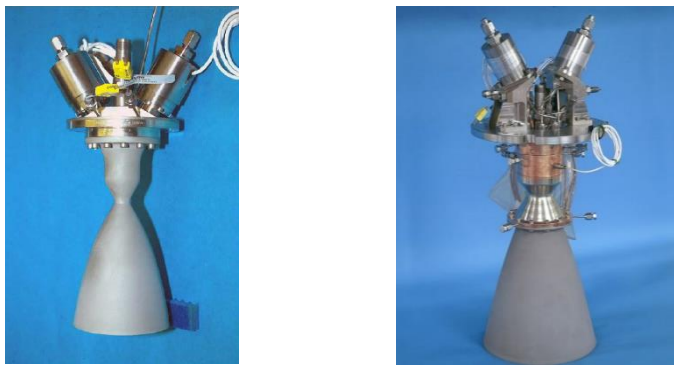
Figure 1.5 Aerojet 100-lbf LOX/LCH4 engine (Left),
Northrop Grumman TR-408 engine (Right) [13]

According to the literature [13], Aerojet developed a 100 lbf class small methane engine through the test data of methane engine developed by modifying LOx / ethanol engine. Liquid methane and oxygen are injected into the combustion chamber by triple impinging injectors, and both the combustion chamber and the nozzle are made of niobium.

According to the above literature, northrop Grumman's TR-408 engine was developed based on engines using hypergolic propellants, and a pintle injector is

installed similar to the TR-308. Methane and oxygen are stored in liquid form in the tank, but since regenerative cooling is applied, both fuel and oxidizer are passed through the cooling channels and fed to the combustion chamber in a gaseous state.

Unlike hypergolic propellants, non-hypergolic propellants require igniter to start combustion. It is important to select an ignition system that is stable and quick to start because small engines may require repetitive restarts depending on their mission. Among the small rocket engines with non-hypergolic propellants, the only engine used in the space missions is NIIMASh's 200N class 17D16 engine used in the Russian reusable spacecraft "Buran", and there are also several test engines based on this engine [15].

According to the article [16], the 17D16 engine uses film cooling with oxidizer, similar to other NIIMash small liquid rocket engines. Gaseous oxygen and liquid kerosene are supplied to the combustion chamber, and a spark type igniter КН-11Б is mounted in the ignition chamber.

Based on this engine, an ethanol engine with a thrust of 235N was developed for accomplishing the same performance of the commercial hypergolic engines [16]. In this engine, the jet injectors supply proper amount of fuel, and the oxidizer sprayed by the swirl injector produces thrust and creates a cooling film on the combustion

chamber wall. Cold test using air and hot test were performed to verify design values according to the article.
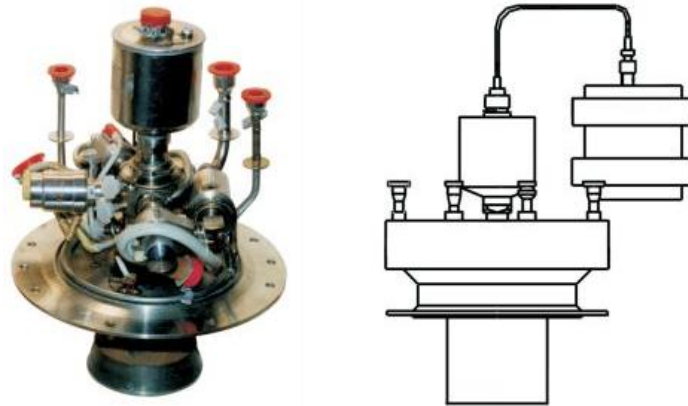
Figure 1.6 17D16 engine for Russian space shuttle "Buran" [11]

NIIMASh's other GOx / Ethanol rocket engines were built with a variety of injection systems [17]. According to the literature, the general structure features of these engines are internal spark ignition systems, ignition chambers and film cooling with fuel. For example, an engine with a thrust of 100N has a fuel jet injector inserted into the oxidizer injector as shown in the figure 1.7. Approximately 50% of the oxidizer is supplied for cooling the spark plug and then participates in the combustion process [17].
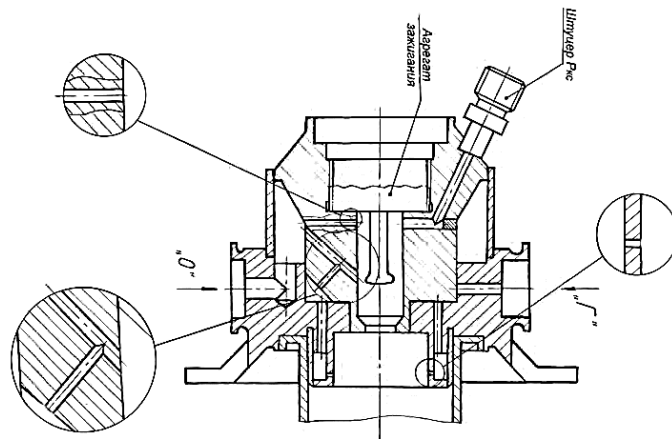
Figure 1.7 Injection system of 100E611 engine [17]

1.3 Objectives

As demand for satellites and space exploration increases, it is necessary to develop high performance small rocket engine. The purpose of this study is to design the injector of 400N class methane rocket engine and to identify the spray characteristics of the injector through cold test. For this purpose, the concept design of the engine was performed first.

A single bipropellant injector has been adopted to simplify the structure. Applying a single injector to the engine has the advantage of reducing the complexity in the development process and reducing the number of machining operations as compared to the multi-injector. As shown in Table 1.1, Europe and Russia have utilized engines with single bipropellant injector for decades

Chapter 2. CONCEPT DESIGN

2.1 Requirements

The development target is an engine for ground testing with a single bipropellant injector to produce a thrust of 400N. The propellant was determined to be oxygen / methane which is efficient and non-toxic. For ground test purposes, 400N thrust is required at the sea level, and nozzle of the engine must be designed considering atmospheric pressure. In addition, due to the characteristics of small rocket engine, the flow rate is small and the chamber pressure is low, so that the supersonic nozzle becomes very short. Therefore, supersonic nozzle for prototype is initially conical shape and can be changed later.

The regenerative cooling and film cooling will be applied to this engine. Unlike Northrop Grumman's TR-408 engine, only methane will be used for regenerative cooling, so gaseous methane and liquid oxygen will be supplied to the combustion chamber. The liquid oxygen fed to the combustion chamber will be used not only for thrust generation but also for film cooling, which is similar to the European and Russian engines presented above.

Electric spark igniter was adopted for this engine because it has low unit cost and

relatively easy to use. A.V. Kochanov and A. G. Klimenko [18] suggested that typical small rocket engines are limited in diameter and the propellant should be reliably supplied to the ignition zone. Further, since the heat shielding of the igniter should be sufficiently performed, it is preferable that the igniter is installed on the top of the injector located on the combustion chamber axis. The 17D16 engine, a small rocket engine using a gas-liquid non-hypergolic propellant mounted on the Buran, is also known to have applied such an ignition system, and the US ethanol engine also used a similar type of igniter [19].

2.2 Combustion chamber design

According to Alemasov [1], injecting propellant, evaporation and combustion take place in the combustion chamber, and all combustion processes are completed in the combustion chamber. The nozzle only accelerates the flow inside the engine supersonic, but the chemical composition changes due to dissociation and recombination. Since the propellant is sprayed into the combustion chamber, which is larger than the injector nozzle, it slows down and the pressure rises for a while. However, it accelerates again by the chemical reaction. The static pressure is lower at the outlet of the nozzle than at the outlet of the combustion chamber because the

flow accelerates in the nozzle. The temperature of the flow in the engine is usually maximized near the nozzle throat, and the static temperature T decreases as the velocity W increases with constant total temperature T_0.
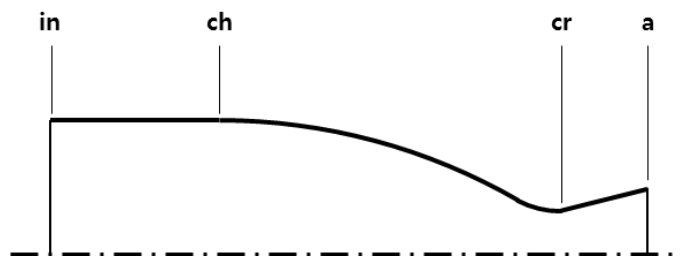
Figure 2.1 Schematic of combustion chamber and nozzle
(In – Inlet of Combustion Chamber, ch – outlet of Combustion chamber,
cr – Nozzle Throat. a – Outlet of Supersonic Nozzle)

In the design process, chamber pressure were set to 1.2 [MPa] based on the previous works. The supersonic nozzle was determined as a conical shape with a half angle of 30 degrees with reference to the literature [21]. Thermodynamic calculations were performed by inputting these initial values to the commercial program RPA. Flow in the nozzle was assumed to be equilibrium. As a result of iterative calculation, the specific impulse was the highest when the O / F ratio was $2.5 \sim 2.7$. Therefore, the O / F ratio was selected as 2.593 ($\alpha = 0.65$), and the specific impulse in this case is 235 sec. This O / F ratio value is similar to the combustion

test results of the Aerojet's methane engine as shown in figure 2.2.
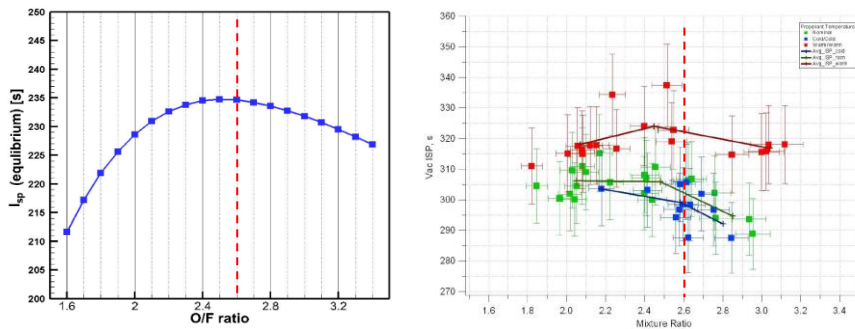
Figure 2.2 Comparison of RPA calculation results (Left) and
hot test results of Aerojet's methane engine (Right) [12]

Thermodynamic calculations of each section of the combustion chamber using

RPA were also performed and are shown in Table 2.1. Figure 2.3 shows the heat flux

and temperature distribution at the wall calculated by RPA. Each maximum value

appears near at the nozzle throat. At a position close to the head, the propellant is

present in an unburned state, so the temperature and the heat flux are considerably

low, but the gradient changes abruptly as the combustion progresses.

The design of the combustion chamber was performed based on the initial value

and the calculated parameters by RPA. According to the recommended value of small

engine [15], the combustion chamber loss factor and nozzle loss factor were 0.94

and 0.97 respectively.

Parameter	Injector (in)	Nozzle Inlet (ch)	Nozzle Throat (cr)	Nozzle Exit (a)
Pressure [MPa]	1.20	1.20	0.69	0.10
Temperature [K]	3250	3249	3071	2180
Gamma	1.17	1.17	1.16	1.23
Isentropic Exponent	1.14	1.14	1.14	1.23
Density [kg/m³]	0.81	0.81	0.50	0.10
Velocity [m/s]	0	77	1254	2461
Mach number	0	0.06	1.00	2.25

Table 2.1 Calculation results by RPA

Figure 2.3 Heat flux (Left), and temperature distribution (Right) calculated by RPA

According to V. M. Kudryavtsev [22], the cross-sectional area of the combustion chamber can be determined by either the contraction ratio or the relative intensity of flow rate. The contraction ratio is the ratio of the combustion chamber cross-sectional area F_{ch} to the nozzle cross-sectional area F_{cr}. If this value is small, the

16

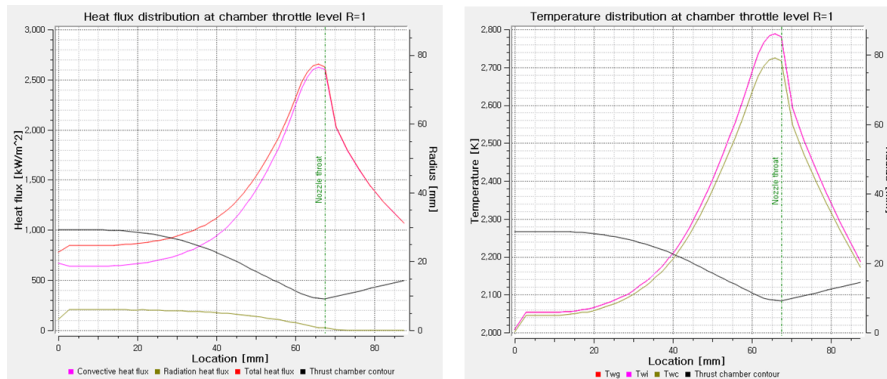mixing process of propellant is complicated, so the selection of the combustion chamber cross-sectional area is limited [34]. On the other hand, the larger the contraction ratio is, the smaller the effect of the propellant momentum is [20]. Also, when the contraction ratio is large, the rate at which thermal energy is converted into kinetic energy increases [35].

The intensity of flow rate is the mass flow rate through the combustion chamber divided by the cross-sectional area. The larger the value, the higher the efficiency of the engine but also the higher the possibility of combustion instability [23-25]. The relative intensity of flow rate is the combustion chamber pressure divided by the intensity of flow rate, and there is a recommended value by experience. According to Kozlov [15], the relative flow intensity $\bar{q}$ for small engines is 4.7×10^{-5} [sec / m]. In this study, the combustion chamber was designed using this value.

$$q = \frac{\dot{m}}{F_{ch}} = \frac{p_{ch} \cdot F_{cr}}{F_{ch} \cdot \beta} = \frac{p_{ch}}{\overline{F_{ch}} \cdot \beta} \left[\frac{\text{kg}}{\text{m} \cdot \text{sec}^2}\right] : \text{Flow rate of intensity}$$

$$\bar{q} = \frac{F_{cr}}{F_{ch} \cdot \beta} = \frac{\dot{m}}{F_{ch} \cdot p_{ch}} \ [\text{sec/m}]: \text{Relative flow rate of intensity}$$

The static pressure coefficient ϵ_k can be obtained from the velocity loss coefficient of the propellant injected into the combustion chamber and the combustion chamber pressure reduction coefficient, and the velocity loss coefficient

of injection can be obtained by the average velocity of propellant w_{cp} given by the following equation. This value varies with the phase of propellant [20].

$$w_{cp} = \frac{K_m}{K_m + 1} \cdot W_{ox} + \frac{1}{K_m + 1} \cdot W_{fu}$$

The length of the cylindrical part of the combustion chamber can be obtained by using the characteristic length L^*. The characteristic length is a value obtained by dividing the volume of the combustion chamber by the cross-sectional area of the nozzle. Assuming that the volume of the combustion chamber is constant, the longer the value of the characteristic length becomes, the shorter the length of the combustion chamber becomes. As a result, it can be said that the characteristic length is proportional to the time of the propellant stay in the combustion chamber.

In this study, characteristic length was firstly chosen as the statistical intermediate value of gaseous hydrogen and kerosene engines because methane has intermediate characteristics of hydrogen and kerosene [15,20,22,26]. In addition, the characteristic length of small engines is generally known to be about 60% of large engines [9, 27], so the characteristic length was set to 0.4 m. In general, the characteristic length of a small engine is known to be 0.4 m ~ 0.6 m [27], so this value seems reasonable. The shape of the designed combustion chamber with nozzle is shown in Figure 2.4.
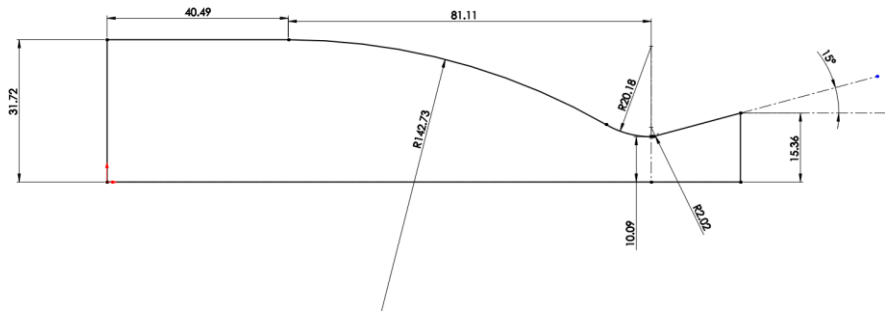
Figure 2.4 Geometry of combustion chamber and nozzle

2.3 Numerical analysis

In the previous design process, performance and parameters of the engine were predicted based on the results of RPA calculation. However, in the calculation process of the RPA, it is assumed that oxidizer and fuel are ideally injected and mixed at the inlet of the combustion chamber and assumed uniform distribution over the cross sectional area, so each parameter is the same along the cross section[22,28]. On the other hand, small rocket engine has a small number of injecting and mixing elements and a small volume of the combustion chamber, so it is difficult for the distribution of the propellant to be uniform along the cross section. In addition, the formula for RPA is based on the theory of large engines. Therefore, the calculated values of RPA may differ from the real parameters of engine. As a result, numerical

analysis with 3D modeling is needed to verify the geometry of the designed combustion chamber.

Previous work [29] has been conducted to understand the effects of geometric parameters of combustion chamber on engine performance and wall heat flux in a small rocket engine under ideal conditions. In this study, as shown in Figure 2.5, a combustion chamber with a straight subsonic nozzle and a bell-type supersonic nozzle with an expansion ratio of 1000 were used. It was assumed that ideally uniform high-temperature flows through the combustion chamber without considering injection and combustion processes. Therefore, this analysis was intended to identify trends, and numerical comparisons are almost meaningless.

According to the literature [15,22], unlike a large engine, the combustion process of small rocket engine is not completed in the cylinder part of the combustion chamber because of the small size of the combustion chamber, and the chemical reaction occurs until the subsonic nozzle. Thus, not only the diameter and length of the cylinder part of the combustion chamber but also the length of the subsonic nozzle were also specified as variables.
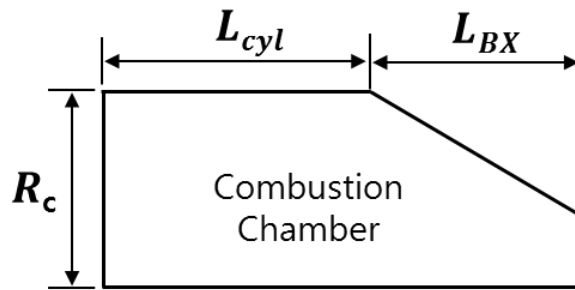
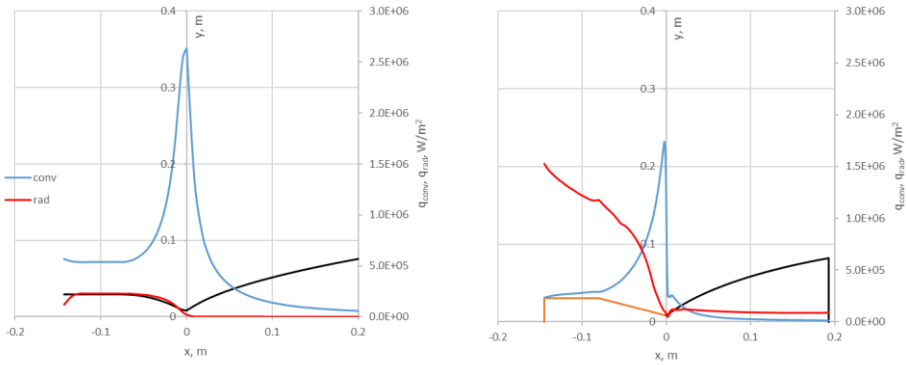Figure 2.5 Geometry of combustion chamber used in analysis [29]

Figure 2.6 Heat flux calculation results by RPA (Left) and 3D modeling (Right) [29]
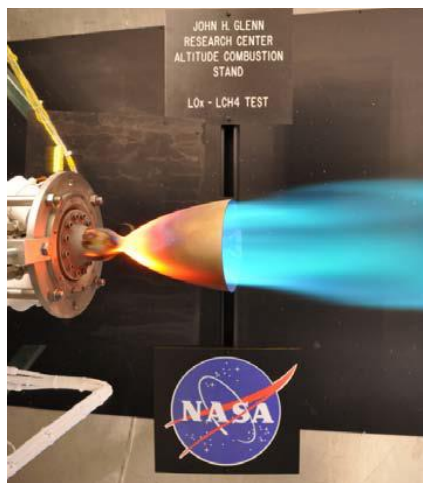

Figure 2.7 Hot test of Aerojet's methane engine [12]

Comparison of the distribution of the heat flux calculated by RPA and the numerical analysis results are as follows. The heat flux distribution calculated by RPA shown in Figure 2.3 shows that most of the heat flux is convective heat flux. On the other hand, as shown in Figure 2.6, the numerical analysis results of the small engine show that the radiative heat flux is larger than the convective heat flux in the cylindrical part of the combustion chamber, and these trends were the same in most of the cases. The results of previous studies show that there is a difference in the results of RPA calculation and 3D modeling of small engines, and the radiative heat flux at the combustion chamber can be a problem. In addition, as shown in Figure 2.7, the hot test image of the Aerojet's small methane engine show that the cylindrical section of combustion chamber walls are heated. Therefore, cooling is necessary to prevent thermal damage to the head and combustion chamber walls in small engines. However, unlike the conditions of this study, where the ideal flow passes through the combustion chamber, the actual small rocket engine is protected by proper cooling method. In other words, in most small rocket engines, the injected propellant lowers the temperature in front of the combustion chamber, and film cooling can be used with fuel or oxidizer. Therefore, the design of the injection system of small rocket engines is important both in the performance and cooling.

The goal of present study is to design the injector of an engine with a single bipropellant injector, so the injector should be selected to be capable of not only generating thrust but also cooling the wall. In order to develop such an injector, it is necessary to refer to an example of an engine using hypergolic propellants. As mentioned earlier, engines such as the S400 and 11D458, which use a single bipropellant injector, are equipped with double swirl injector and are film cooled with oxidizer. However, since methane engines differ in temperature, chemical characteristics, and phase of propellant from conventional engines, additional studies on the proper type of injector are required, so numerical analysis is conducted.

Bipropellant injector is composed of a combination of an oxidizer and a fuel injector, so the atomization and mixing process of the spray may vary depending on the combination type as well as the design of the individual injector. Some injectors for gas-liquid propellant can be considered. Injector types commonly used in general rocket engines include jet injectors and swirl injectors, and there are several representative combinations for application to gas-liquid propellants. An example is the injector of the RD-170 engine used in the first stage of Energia as shown in figure 2.8. It is a combination of an internal gas jet injector and an external liquid swirl injector [30]. However, since the large engine RD-170 and the small methane engine

are different from each other in the number of the injector element and the characteristics of the propellant, there is a possibility that a suitable injector for small methane engine may be different. For example, the position of the gas injector and the liquid injector can be exchanged, and since the volume of the combustion chamber of the small rocket engine is small, the use of a gas swirl injector instead of a gas jet injector can be considered. Therefore, we can think of the four combinations of coaxial injectors as follows: inner gas jet and outer liquid swirl (A), inner liquid swirl and outer gas jet (B), inner liquid swirl and outer gas swirl (C), inner gas swirl and outer liquid swirl (D) injectors.
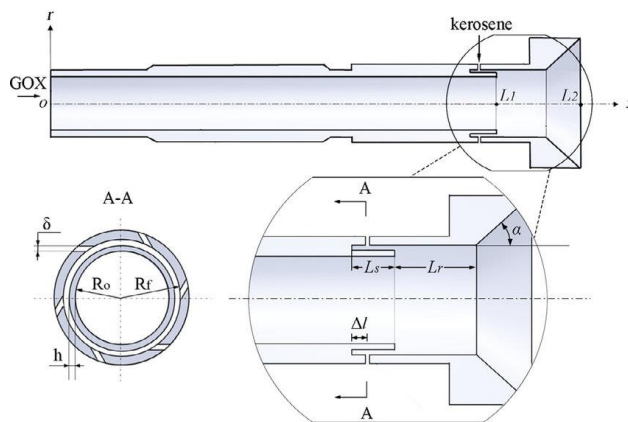
Figure 2.8 Schematic of injector of the RD-170 engine [30]

In order to select an appropriate injector, numerical analysis were performed to identify the differences in engine parameters according to the type of injector. Unlike the previous study, where the uniform high temperature flow passes through

24

a simplified combustion chamber, the shape of the designed combustion chamber

was used for the analysis and the droplet combustion model is additionally applied.

Figure 2.9 Geometry for numerical analysis of combustion chamber
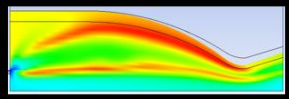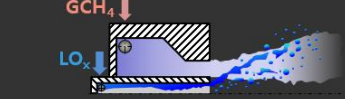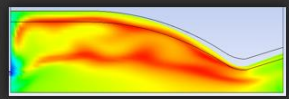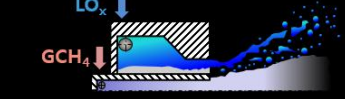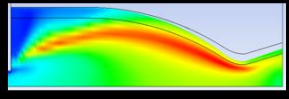
Figure 2.10 Comparison of injector types by numerical analysis

ANSYS CFX, a commercial program, is used for numerical analysis. Modeled geometry is divided into three parts: Ambient, Wall, and Combustor as shown in Figure 2.9. Mesh was scaled considering the boundary layer. The initial values of the inlet and outlet conditions are applied with the temperature, pressure and the kind of molecules predicted by the RPA.
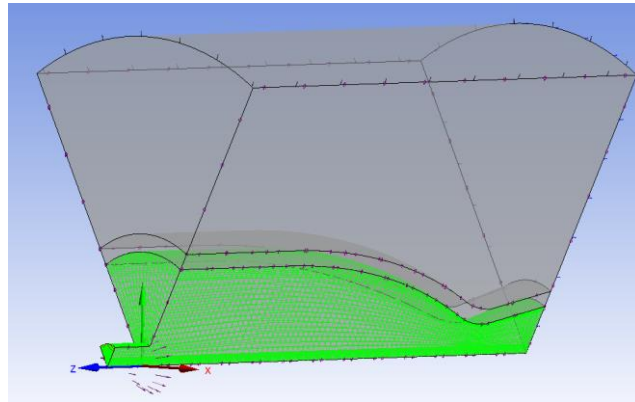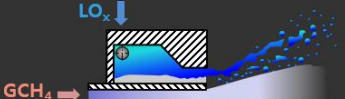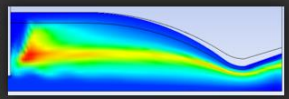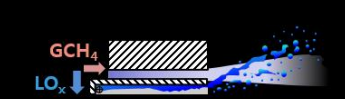
Analytical model of each domain is applied with reference to the literature [31] for the numerical analysis of the rocket engine. Total energy was used for the heat transfer model. Shear stress transport was used for the turbulence model, and Monte Carlo model was used for the thermal radiation. At the entrance of the combustion chamber, supposing that the injector is installed, the gas and the droplet are injected at the speed and diameter assumed by theory. Therefore, the diameter of the droplet is constant, and the CAB model is applied as the breakup model. Ranz Marshall model was used for the heat transfer model, so the droplets are evaporated. The combustion model assumes a single step reaction. The coefficient of the reaction equation is determined using the chemical equilibrium calculation result of RPA. The Eddy dissipation model is applied as the combustion model. The result of the analysis through this method is shown in Figure 2.10.

Type (A) is an injector in which a gas jet injector is located inside and a liquid swirl injector is located coaxially to the outside. Figure 2.11 shows that a significant amount of oxidizer and fuel are not mixed with each other in this case. Therefore, there are a large amount of propellants that escape without burning, and thrust and specific impulse are low.
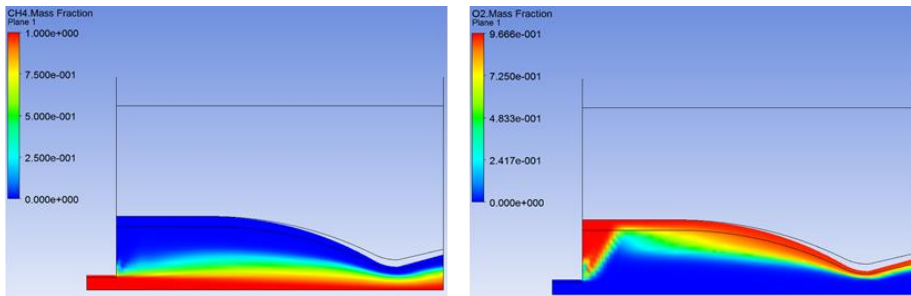
Figure 2.11 Distribution of propellant when type (A) injector is applied
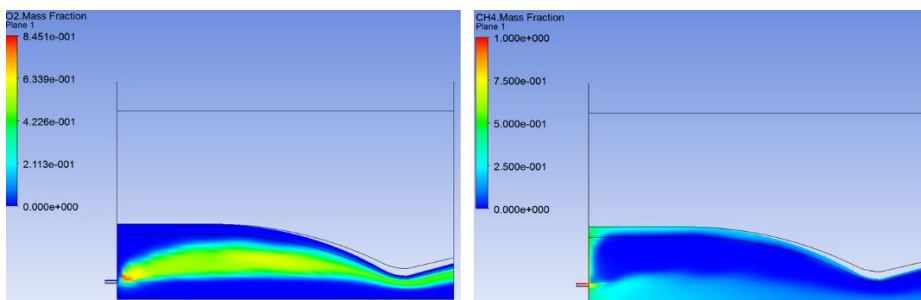
Figure 2.12 Distribution of oxygen when type (B) injector is applied (Left) and distribution of methane when type (C) injector is applied (Right)

Type (B) is an injector in which the position of the liquid and gas injector are reversed, and gas jet collide with the liquid cone. Thus, although the mixing efficiency is improved, the amount of propellant still escapes due to the fast axial velocity of the gas jet, and a high momentum liquid flow penetrates the jet and burns near the wall as shown in Figure 2.10 and 2.12. In this case, although the mixing efficiency is improved, the temperature distribution becomes inappropriate.

Type (C) is a type (B) injector in which the external gas jet injector is replaced by a swirl injector. It has the highest mixing efficiency and thrust among the four cases. On the other hand, high temperatures at almost all locations in the combustion chamber due to high mixing efficiency are a drawback in wall cooling. Although the methane pushed up to the wall makes a little fuel rich layer, it is not enough to cool the walls of the combustion chamber, as shown in Figures 2.10 and 2.12.

Type (D) is an injector in which the position of the liquid and gas injectors in the injector of type (C) is reversed. The mixing efficiency of the injector is slightly lower than the type (C), because the gas spray is hard to penetrate the outer liquid film, as shown in Figure 2.13. However, this causes the oxygen-rich region near the wall to lower the wall temperature, and this cooling mechanism is similar to conventional engines using oxidizer film cooling. Also, since both the liquid and the gas injectors

are swirl injectors, combustion efficiency and performance of the engine does not

drop significantly.
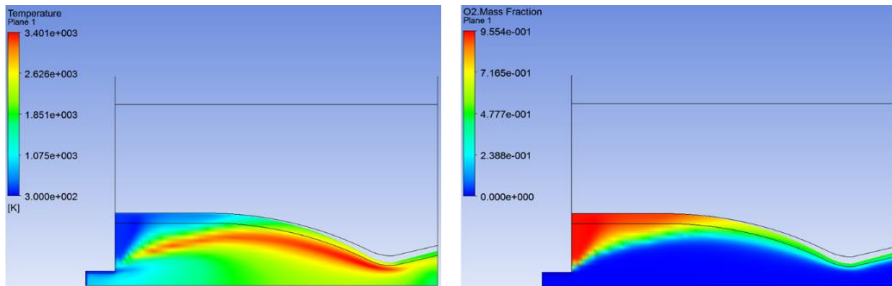
Figure 2.13 Distribution of temperature (Left) and oxidizer (Right)
when type (D) injector is applied
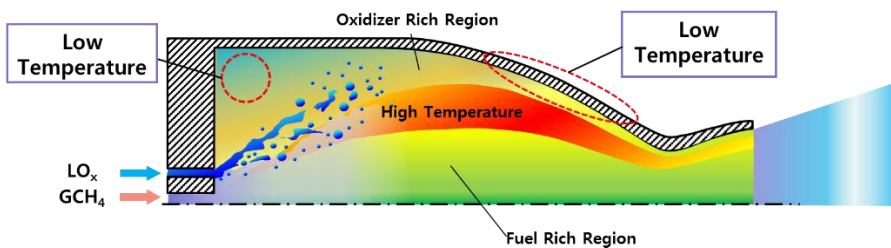
Figure 2.14 Schematic of engine with type (D) injector

In the fluid-dynamic 3D modeling, it is assumed that the droplet is injected at a

fixed size, so the results of the analysis may be different from the actual value, but it

can be used to get a tendency. Numerical results show that the injector type (D) is

advantageous in both performance and cooling of the engine. Therefore, it is

considered that the type (D) injector can be used to generate thrust and cool the engine simultaneously, even when used as a single injector. Thus, Type D injectors have been adopted and, consequently, it is similar to injectors of existing engines using single injectors.

2.4 Injector design

In order to overcome the disadvantages of the numerical analysis, it is necessary to experimentally verify the injector. In this study, spray characteristics were obtained through cold test as the first step.

According to the literature [32], it is considered that the process from injection of propellant to primary atomization is least influenced by propellant reaction during the combustion process. Moreover, in coaxial injectors using oxygen / hydrocarbon propellants, the reaction time will be slower due to evaporation and mixing, so the reaction will have less effect on atomization than impinging injectors that use a storable propellant. Therefore, the cold test is an efficient method that can understand the spray characteristics without expensive and complex apparatus for hot test.

The spray characteristics of the coaxial injector are strongly influenced by the interactions of two individual injectors. One of the most important parameter for

determining the interaction of the two injectors is the difference in momentum between the fuel and oxidizer. In addition, spray angle of the two injectors is a representative factor that changes the difference in momentum between the fuel and oxidizer, and affects the mixing and distribution of the propellant. As shown in the numerical analysis results, the distribution of the propellant caused by single coaxial injector has a great influence on the engine characteristics due to the small number of spray elements in the engine. Therefore, proper adjustment of the spray angle is important in the design of small engine

By this reason, initial values of the injector design were set as the spray angle and injection pressure drop. In addition, the expansion coefficient, the number of inlet channels, and the mass flow rate calculated by RPA were input.

2.4.1 Design of liquid injector
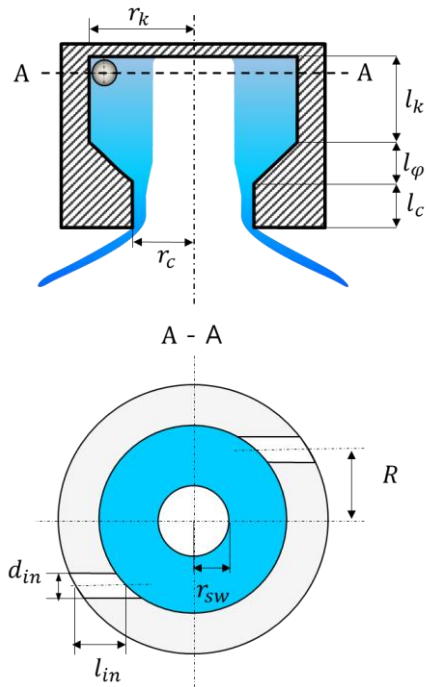
Figure 2.15 Schematic of liquid injector

Liquid injector is designed by the modified methodology of Kesaev [36] and Dityakin [37]. This theory first assumes an inviscid condition and describes the behavior of the fluid inside the injector, and then applies more realistic conditions. The following explanation is based on this theory.

According to the theory, liquid rotating inside the swirl chamber has a gas vortex

at the center, and the liquid occupies only a part of the nozzle cross section. Therefore, the ratio of the liquid occupied is expressed by the coefficient of passage fullness φ, and when the flow rate is constant, the coefficient is inversely proportional to the axial velocity.

$$\varphi = 1 - \left(\frac{r_{sw}}{r_c}\right)^2 : \text{ Coefficient of passage fullness}$$

The coefficient of nozzle opening is the ratio of the radius of the swirl chamber to the radius of the injector nozzle. When this value is larger than the critical coefficient of nozzle opening C_{cr}, it is called an close type injector, and when it is smaller, it is called an open type injector. It is generally known that close type injectors are suitable for injectors with small flow rates and that the non-uniformity due to the number of tangential flow paths is reduced. For this reason, the liquid injector was selected as close type.

The geometrical characteristic coefficient is a parameter related to the shape of the injector. As this value increases, the entrance channel becomes narrower and the swirl chamber becomes thicker. Therefore, as the geometrical characteristic coefficient increases, the tangential velocity increases and the axial velocity decreases.

$$A = \frac{R \cdot r_c}{r_{in}^2} = \frac{F_c \cdot R}{F_{in} \cdot r_c} : \text{Geometrical characteristic coefficient}$$

The discharge coefficient is the ratio of the actual flow rate to the theoretical

maximum flow rate and is expressed in terms of φ.

$$\mu_\phi = \frac{1}{\sqrt{\dfrac{1}{\varphi^2} + \dfrac{A^2}{1 - \varphi}}} : \text{ Discharge Coefficient}$$

Based on these variables, the liquid spray angle injected under inviscid conditions

when considering the dynamic pressure due to the central gas vortex of the liquid is

as follows.

$$\tan \bar{\alpha} = \frac{2A \cdot \mu_\phi}{\sqrt{(1 + S)^2 - 4A^2 \cdot \mu_\phi^2}}$$

$$S = \frac{r_{sw}}{r_c}$$

However, since there is viscous friction in the actual fluid flow, angular

momentum decreases and the spray angle decreases as compared with ideal

conditions. To obtain the spray angle when there is friction force, the geometrical

characteristic coefficient and the discharge coefficient are redefined considering the

viscosity.

$$A_{eq} = \frac{(1 - \varphi) \cdot \sqrt{2}}{\varphi \cdot \sqrt{\varphi}}$$

: Equivalent geometrical characteristic coefficient under viscous conditions

$$\mu'_\phi = \cfrac{1}{\sqrt{\cfrac{A^2_{eq}}{1-\varphi} + \cfrac{1}{\varphi^2}}}$$: Discharge coefficient under viscous conditions

In addition, spray angle under viscous conditions are redefined through the spray angle under the inviscid conditions and the equivalent geometrical characteristic coefficient.

$$\bar{\alpha}' = \arctan\left[\cfrac{2 \cdot A_{eq} \cdot \mu_\phi}{\sqrt{(1+S)^2 - 4A_{eq}^{\;2} \cdot \mu_\phi^2}}\right]$$: Spray angle under viscous conditions

When there is a viscosity in the liquid, not only the angular momentum is reduced but also the pressure drop due to the friction and the shape of the flow path occur in each part of the injector. In the calculation process for the injector design, this loss is divided into energy loss at the tangential inlet Δ_{in}, energy loss inside the swirl chamber Δ_k, energy loss due to swirl chamber length Δ_L, and energy loss between swirl chamber and injector nozzle Δ_{noz}. In addition, total energy loss is obtained by adding each factor. The newly defined discharge coefficient by this energy loss factor is as follows.

$$\mu'_\phi = \cfrac{1}{\sqrt{\cfrac{A^2_{eq}}{1-\varphi} + \cfrac{1}{\varphi^2} + \Delta_\Sigma}}$$: Discharge coefficient considering energy loss

$$\Delta_\Sigma = \Delta_{in} + \Delta_k + \Delta_L + \Delta_{noz}$$: Sum of energy loss factors

In this study, an algorithm was developed to obtain the desired spray angle by modifying the equation based on these theories. Therefore, initial value is the spray angle, and the injector is designed by adjusting the dimension of each part while considering the structural effect on spray characteristics. The geometry of the designed injector is as follows.
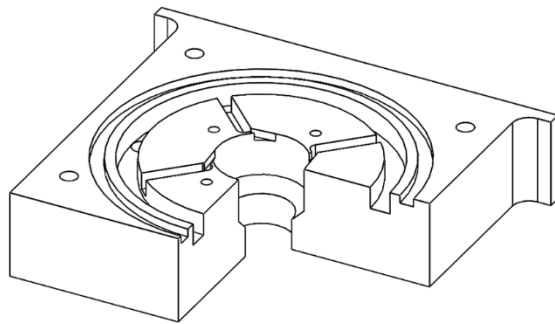
Parameter	Length (mm)
r_k	12.99
r_c	9.26
r_{in}	1.70
l_k	12.99
l_φ	3.73
l_c	9.26
l_{in}	5.43

Figure 2.16 Geometry of designed liquid injector
(A portion of the drawing was cut for cross-sectional display.)

2.4.2 Design of gas injector
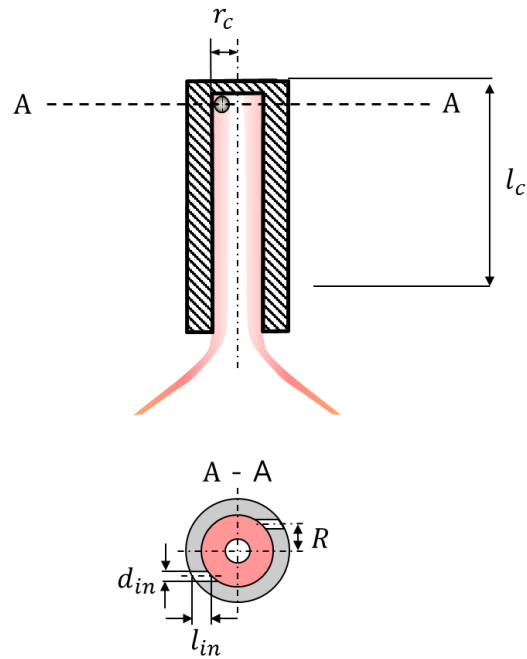
Figure 2.17 Schematic of gas injector

Since the gas injector is located inside the liquid injector, the igniter is inserted at the top. It is known that when the igniter is installed on top of the close type injector, there is a risk of the flame being reflected from the nozzle, causing the injector to explode. Therefore, the gas injector was selected as the open type.

Gas injector is designed by Russian standard method (GOST 21980-76) and the

theory of Vigor Yang [38]. Following explanation is based on them. Since the gas is a compressible fluid, there is a change in the design equation and the temperature at the inlet is added to the initial value. The key equation used in the design of the gas injector is given below.

$$Re_{in} = \frac{4}{\pi\sqrt{2}} \cdot \frac{\dot{m}_\Phi}{\mu\sqrt{d_c}} \cdot \sqrt{\frac{A}{R}} \quad : \text{Re number in tangential inlet}$$

$$\dot{m}_\Phi = \sqrt{2}d_c \cdot \frac{\mu_\Phi \cdot p_{out} \cdot \varphi_\Phi}{\mu\sqrt{RT_{in}}} \cdot \sqrt{\frac{A}{\bar{R}}} \quad : \text{Mass flow rate of the injector}$$

$$d_c = \sqrt{\frac{4}{\pi\sqrt{2}}} \cdot \sqrt{\frac{\dot{m}_\Phi\sqrt{RT_{in}}}{\mu_\Phi \cdot p_{out} \cdot \varphi_\Phi}} \quad : \text{ Radius of nozzle of the injector}$$

$\bar{R} = R/r_c$, φ_Φ is a variable for calculation and is given by the following equation.

$$\varphi_\Phi = \frac{p_{in}}{p_{out}} \cdot \sqrt{\frac{k}{k-1}\left(\frac{1}{\left(\frac{p_{in}}{p_{out}}\right)^{\frac{2}{k}}} - \frac{1}{\left(\frac{p_{in}}{p_{out}}\right)^{\frac{k+1}{k}}}\right)}$$

The gas injector also forms a vortex of external gas inside the rotating propellant. During design process, the two fluids are separated based on when the axial velocity is zero. However, in actual injector, the two gases are mixed with each other and the boundary is expected to be blurred.

The average spray angle is determined based on the plane with the maximum velocity. A gas injector was designed with reference to this basic theory and the relationship between the structural dimensions of the injector. The geometry of the injector is shown in Figure 2.18.

Parameter	Length (mm)
r_c	5.41
r_{in}	1.5
l_c	36.8
l_{in}	4.35
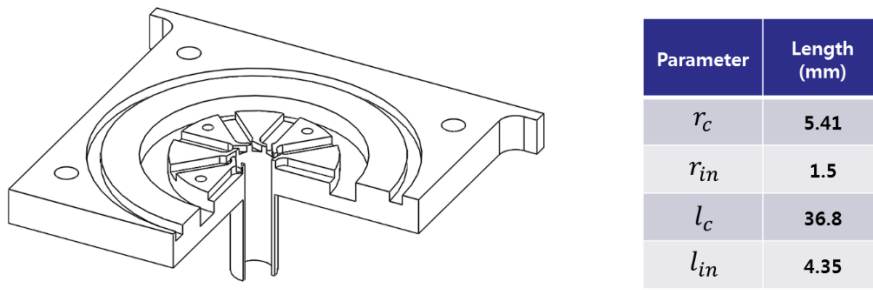
Figure 2.18 Geometry of designed gas injector
(A portion of the drawing was cut for cross-sectional display.)

2.4.3 Design of coaxial injector

According to Vigor Yang [38], the coaxial bipropellant injectors for liquid rocket engines can be divided into two types: external mixing and internal mixing. External mixing is the case where the mixing of two propellants occurs outside the injector. In internal mixing, the spray cone of inner injector collides with the wall of the outer injector. Following explanation is based on the above literature

There are two design methods for external mixing, one of which is the case where the inner injector is located in the gas vortex of the outer injector. In this case, the two injectors are independent of each other, and the geometrical characteristic coefficient is calculated by using the difference of the spray angle of the two injectors. Then, the inlet flow path and the diameter of the nozzle of each injector are calculated. Finally, the injector is designed by repeating confirmation that the condition of Re number is satisfied.

The other is the case where the nozzle of the inner injector invades the liquid film of the outer injector. In this case, the diameter of the nozzle should be increased to compensate for the reduced flow rate without changing the injection pressure drop and the spray angle. Therefore, the discharge coefficient is proportional to $r_{c,out}/r_{c,in}$. The design method in this case is to calculate the outer nozzle diameter of the inner injector, and then determine the nozzle diameter of the outer injector such that a suitable gap is obtained. And then confirms whether the injection pressure drop of the outer injector satisfies the desired condition. The injection pressure drop is obtained using the following formula.

$$\Delta p_{in,out} = \frac{0.05\dot{m}_{in,out}^2}{\mu_{out}^2 \rho_{out} r_{c,out}^4}$$
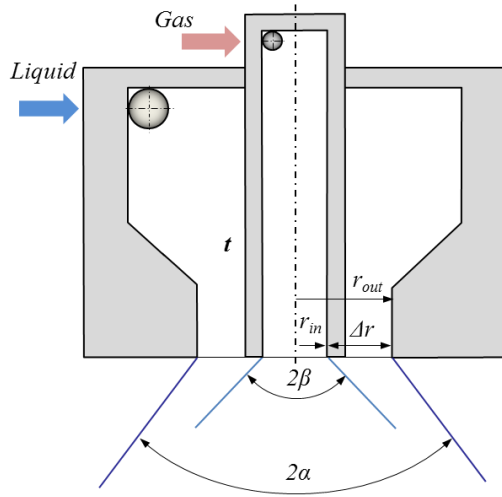
Figure 2.19 Schematic of external mixing injector

- **Lip thickness : t**
- **Recess length : L_r**
- **Length of mixing zone : L_{mix}**
- **Recess number :**

$$RN = \frac{L_r}{L_c}$$

- **Contact Length :**
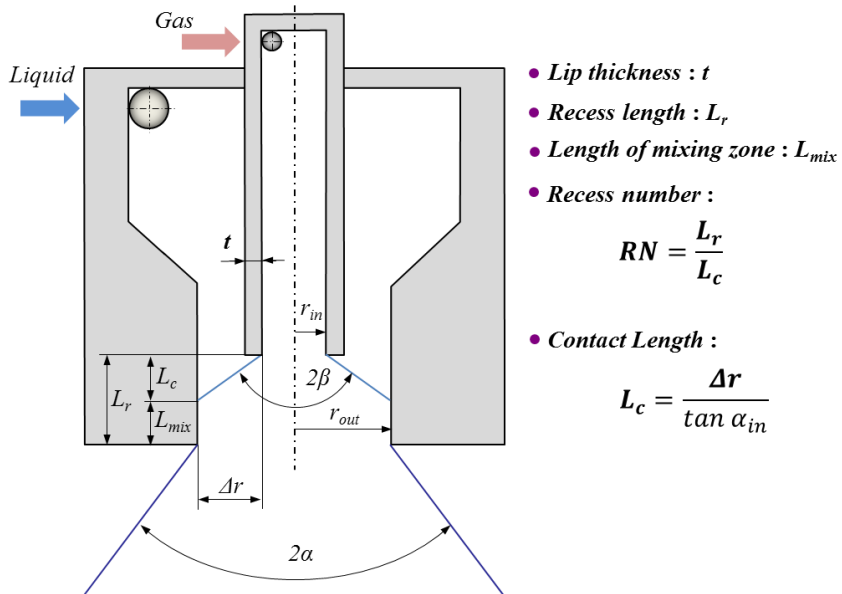
$$L_c = \frac{\Delta r}{\tan \alpha_{in}}$$

Figure 2.20 Schematic of internal mixing injector

In the internal mixing injector, the propellant sprayed from the inner injector is mixed in the nozzle of the outer injector. This is because the inner injector of the coaxial injector was retracted to a certain distance from the injector head surface as shown in Figure 2.20. Generally, injectors of engines using non-hypergolic propellants apply a premixed section called a recess to increase ignition and combustion efficiency.

The length of the mixing zone is the distance from the point where the spray of the inner injector collides with the wall of the outer injector to the outlet of the outer injector. It determines the residence time of the mixed propellant in the injector.

The residence time should be set within a reasonable range that permits sufficient mixing and does not detonate the injector. It is known that the recommended value depends on the type of propellant and the flow rate of the injector, and the appropriate residence time increases as the flow rate of the propellant increases. For non-hypergolic propellants, the recommended value of residence time is 0.5×10^{-3} sec when the total propellant flow rate is 0.5 ~ 1.0 kg / sec. The specific impulse increases until the residence time increases to 1.0×10^{-3} sec. However, if the residence time increases further, the specific impulse is constant until the injector explodes. When designing the injector, the residence time is assumed to be

$0.1{\sim}0.5\times10^{-3}$sec. Finally, it is determined by hot test of the engine.

In the case of a liquid-liquid injector, it is possible to predict the velocity of propellant in the injector and reflect the recommended value of the residence time in the design process. However, in the case of gas swirl - liquid swirl injector, it is difficult to predict the velocity of the propellant because two propellants with different phases are rotating inside the injector. Therefore, in this study, the recess length was determined by other methods.

Kim et al. [2] analyzed spray characteristics according to recess length in the case of external mixing, tip mixing, and internal mixing. External mixing and internal mixing are the same as mentioned above. In tip mixing, the spray cone of the inner injector contacts the nozzle outlet of the outer injector. Yang and Ge [39] also classified the recess lengths in the same way, and the tip mixing case was called critical mixing. In these three cases, the mixing mechanism of the propellant is different, and it is expected that the spray characteristics will be significantly different. Therefore, the recess number was selected as 0, 1, and 2 with reference to the above papers, and the differences in spray characteristics of each case were investigated through the cold test.

As mentioned above, the spray angle of the propellant has a large influence on the

operation process of the small engine. For this reason, experiments were carried out to observe spray and atomization characteristics of the coaxial injector with varying liquid spray angle while the gas spray angle was fixed. This is because the gas spray angle is almost unchanged even if the design parameters are changed. Also, the liquid spray angle is relatively easy to be changed by geometric parameters.

According to Kesaev and Vigor Yang [36, 38], in the swirl coaxial injector, when the wall of the inner injector invades the liquid film of the outer injector, the spray characteristics is affected by the ratio between the outer diameter of the inner injector and the radius of the outer liquid film surface. That is, as the lip thickness increases under the same design conditions, the outer liquid spray angle decreases.

Therefore, the lip thickness t and the recess length L_r were determined as parameters affecting the interaction between the gas and liquid injector.

Chapter 3. EXPERIMENTAL METHOD AND APPARATUS

3.1 Experimental conditions

To characterize the coaxial gas-liquid injector, it is necessary to derive the spray characteristics of the individual injector, and the spray angle of the inner injector is required to determine the recess length based on the recess number. Therefore, the spray angle of the gas injector was measured, and experiments were also carried out to find out the effect of lip thickness on liquid spray angle.

To understand the change of spray characteristics of coaxial injector according to the geometry of injector, 9 cases shown in the Table 3.1 were defined. There are three cases for each variable. In the case of lip thickness, the experiment was performed when the spray angle of the liquid was larger, smaller or parallel to the spray angle of the gas. The recess lengths are determined according to whether the start position of mixing is inside the injector or near the exit or outside. It is expected that different types of mixing and break up processes will appear in each case. To find out the

effects of recess length on spray characteristics, injectors with different nozzle

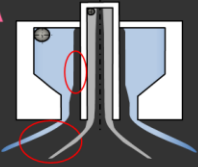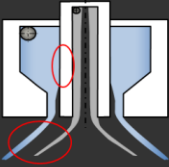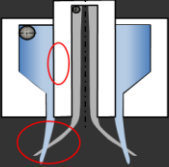lengths were manufactured and combined with a gas injector.
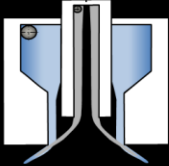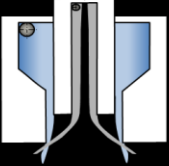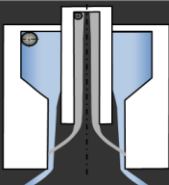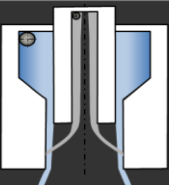
	Non-Impinging (A)	Parallel (B)	Impinging (C)
No Recess $(RN = 0)$	0A	0B	0C
Shallow Recess $(RN \approx 1)$	1A	1B	1C
Deep Recess $(RN \approx 2)$	2A	2B	2C

Table 3.1 Experimental conditions

Hollow cylinders with multiple outer diameters have been used to change the lip

thickness as shown in Figure 3.1. The purpose of this tool is to examine changes in

spray angle and spray characteristics while changing the lip thickness from when the

cylinder does not touch the liquid film until it invades the liquid film. Each cylinder

has a screw thread inside it so that it can fit into the gas injector nozzle. Therefore,

the inner diameter of the cylinder corresponds to the outer diameter of the gas

injector nozzle, and the outer diameter of the cylinder was determined based on the calculation of the internal liquid film thickness of the outer injector. In other words, outer wall of the cylinder was located before and after the expected position of liquid film surface to investigate the change of the spray angle according to the relationship between the liquid film and the inner injector. As a result, lip thicknesses were determined as 3 mm, 3.2 mm, 3.4 mm, 3.6 mm, and 3.8 mm, respectively.

Figure 3.1 Hollow cylinder for changing the outer nozzle diameter of gas injector

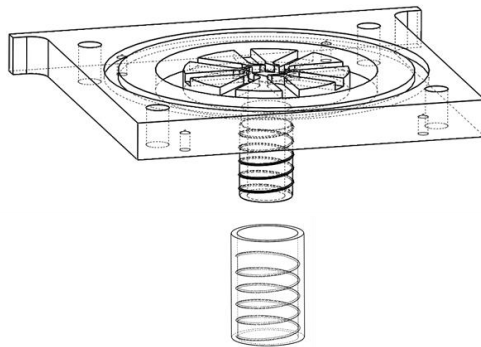According to the design and test experience of a Russian company NIIMash, it is necessary to maintain the pressure drop for balance between the supply system and the combustor, so the injection pressure drop of all experiments was the nominal value. That is, the injection pressure drop of liquid injector was 2.3bar and the gas injector was 6.5bar.

3.2 Water and air supply system

If the actual propellant is used in a cold test, there is a risk of an explosion by propellant that accumulates without burning during the experiment. Thus, the working fluid has been replaced by a simulant. According to the literature [40], water is a valid simulant of LOx in a cold test condition, so water and compressed air replaced liquid oxygen and gaseous methane, respectively. Two pressure vessels were used in the experiment. One of the two was filled with water and the other was filled with pressurized air from the compressor. The water filled vessel was also pressurized with compressed air. Each vessel was equipped with a pressure sensor. A Controller was installed between the compressor and the vessels to control the pressure of the vessels and whether the supply valve is open or closed. The injector was installed in the test rig, and pressure gauges were installed in front of the manifold to compensate for friction losses.

3.3 Optical equipment

DSLR camera (Canon EOS 7D) with a Canon EF 180mm f/3.5L MACRO LENS and a stroboscope (SUGAWARA MS-230DA) was used to observe the characteristics of liquid injector and coaxial injector.

In the case of a gas injector, it is difficult to observe the air. Therefore, in order to visualize the spray of the injector, two mirrors with a diameter of 300 mm and a Canon EOS 7D camera were used to capture the schlieren image. Since the injected air shows a very irregular shape due to turbulence, it is difficult to distinguish the spray angle. So, 500 images taken over time were accumulated to get an average image. The spray angle of the liquid and gas was determined based on the intensity in the averaged spray image using the LaVision SprayMaster program. The liquid spray angle was obtained by accumulating 100 images.

Chapter 4. RESULT AND DISCUSSION

4.1 Characteristics of gas injector

Measuring the spray angle of a gas swirl injector is important in analyzing the interaction of the two propellants through the difference from the liquid spray angle and determining the recess length. The spray image taken by the schlieren technique are shown in Figure 4.1. The accumulated image and measured spray angle are presented together. Under nominal conditions, the spray angle $2\beta_{ex}$ was 80 deg, which is smaller than the design value of 90 deg.
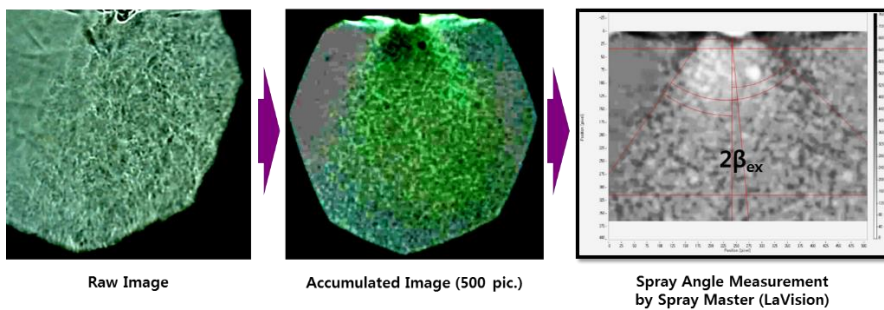
Figure 4.1 Spray angle measurement of the gas injector

4.2 Characteristics of liquid injector

Experiments were performed to analyze the characteristics of the liquid injector without injecting gas in order to investigate the change of the flow characteristics of the liquid injector according to the lip thickness of the internal injector.
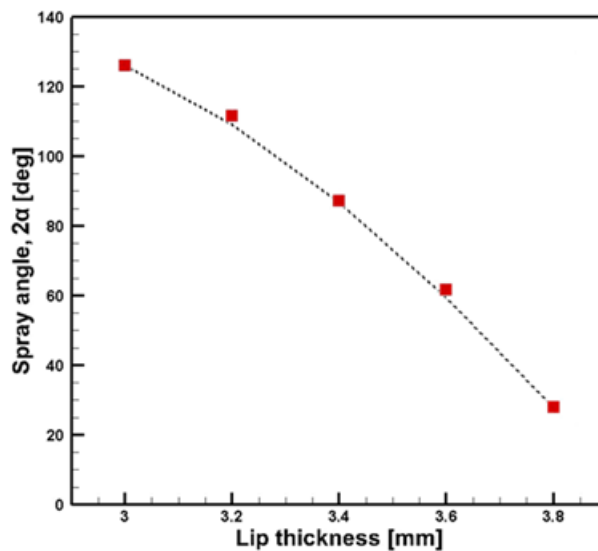
Figure 4.2 Relationship between lip thickness and spray angle

Figure 4.2 shows the change of the liquid spray angle according to the lip thickness. The spray angle decreased with increasing lip thickness. When the lip thickness was 3mm, the liquid spray angle was similar to the design value, and at 3.4mm, the liquid spray angle was similar to the gas spray angle. Therefore, the lip thicknesses corresponding to the experimental conditions of non-impinging, parallel and

impinging shown in Table 3.1 are 3.0, 3.4 and 3.6 mm, respectively.

Figure 4.3 shows the spray image of the liquid injector taken at the three lip thickness conditions. When the lip thickness was 3.4 mm, the axial velocity was considered to be faster because the spray angle was smaller than when the lip thickness was 3.0 mm. Thus, the position at which the liquid film broke into droplets was further away from the injector head. On the other hand, when the lip thickness was 3.6 mm, the liquid film thinned by the inner injector wall was torn from near the head. Therefore, the point at which the liquid film broke into the droplet or ligament was variable, and sometimes the atomization occur closer to the head than when the lip thickness was 3.4 mm. When the lip thickness was 3.8 mm, the gas injector almost completely blocked the nozzles of the liquid injector, so that the angular momentum of the liquid almost disappeared and the spray became very uneven.
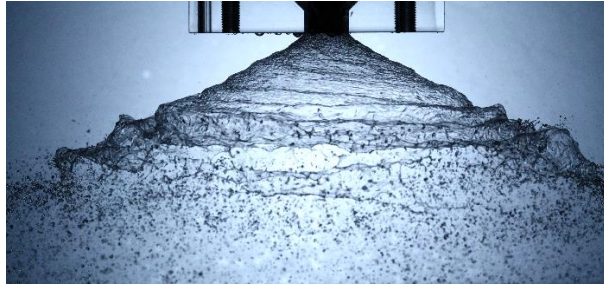
3.0mm
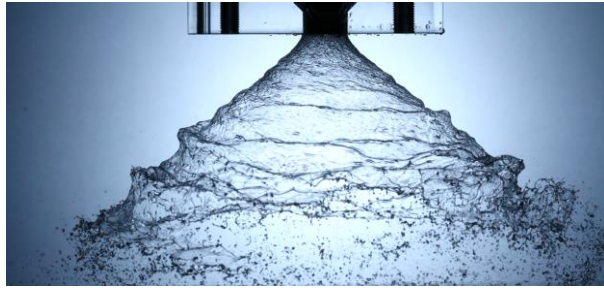
3.4mm
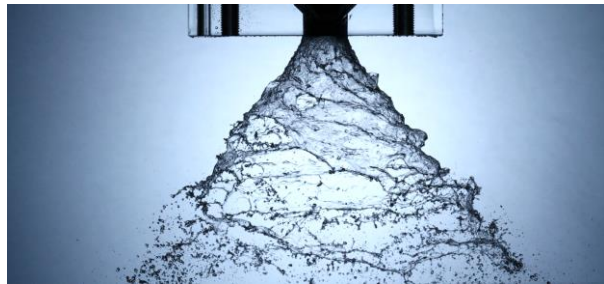
3.6mm

Figure 4.3 Spray images of the liquid injector when the lip thickness of the gas injector is 3.0 mm, 3.4 mm and 3.6 mm

Figure 4.4 Spray images of the liquid injector when the lip thickness of the gas injector is 3.8 mm

As the lip thickness of the gas injector increases, the liquid injector nozzle exit is blocked, so the experiment was conducted to investigate the change of the mass flow rate with the change of lip thickness. Experimental results show that the flow rate decreased with increasing lip thickness. However, when the lip thickness was 3.6mm, the cross sectional area of the outlet of the liquid injector decreased by 91%, but the mass flow rate decreased only by 5.8% compared to 3.0mm. This seems to be due to the increase in the axial velocity of the liquid by the reduction of the spray angle when the lip thickness increases. In case of Lip Thickness of 3.8mm, which showed abnormal spray pattern, the flow rate decreased sharply. In addition, the flow rate was similar to the design value of 128.65 g/s in most of the cases of lip thickness, except when the lip thickness was 3.8 mm.

Lip Thickness (mm)	Mass Flow Rate (g/s)	Area of Liquid Injector Exit (mm^2)
3.0	131.4	2.32
3.2	129.0	1.37
3.4	127.4	0.66
3.6	123.8	0.21
3.8	28.7	0.01

Table 4.1 Mass flow rate of the liquid injector according to the lip thickness of the gas injector

4.3 Characteristics of coaxial injector
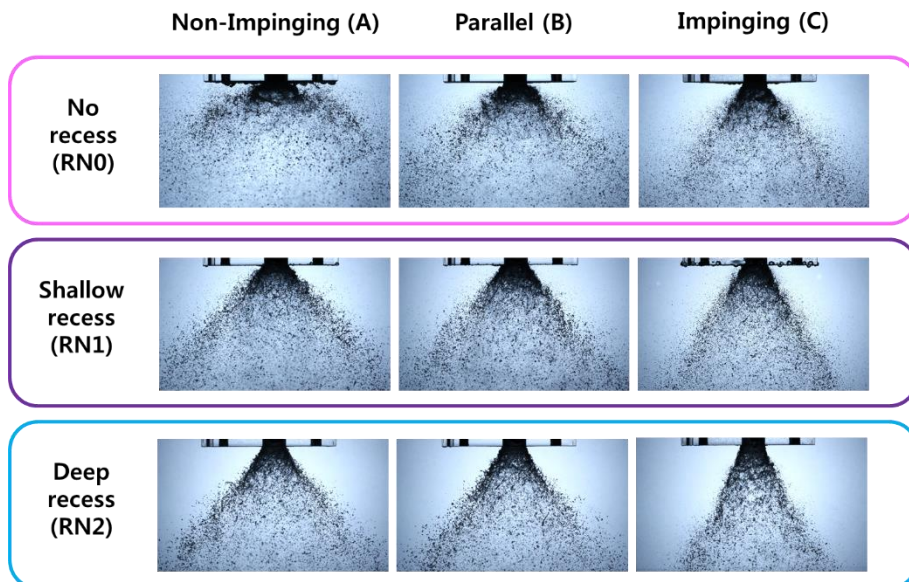
Figure 4.5 Spray characteristics in all cases

4.3.1 No recess

In the case of external mixing, spray characteristics was observed when the selected three lip thickness were applied. In the case of parallel, although the spray angle of the gas and liquid of the individual injectors was close to parallel, they are encountered by entrainment rather than proceeding side by side.

Comparing the three cases, it was impinging case that the size of the droplet is relatively small and uniform. Also, as the lip thickness increased, fluctuation of mass distribution was reduced. In the impinging case, the liquid film was most affected by the momentum of the gas because the two spray cones meet each other. Therefore, it is presumed that atomization occurred efficiently and uniformly, so the mass flow was not concentrated at one point and the change in the mass distribution is small.

Figure 4.6 Fluctuation of mass distribution in non-impinging case

4.3.2 Shallow recess

The shallow recess was designed such that the spray cone of the gas contacts the outlet of the liquid injector (RN = 1), and the deep recess was designed to have the recess length twice that of the shallow recess. However, since the gas is injected i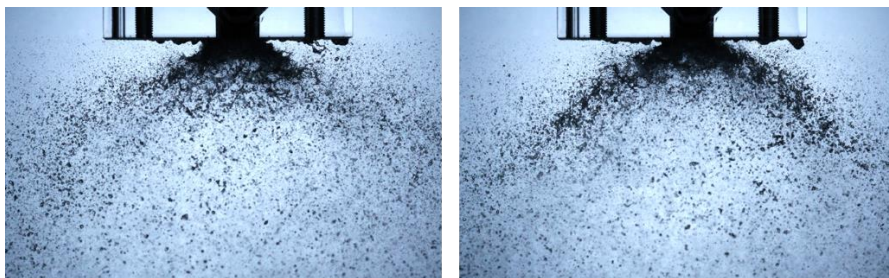nto the liquid injector nozzle, mixing of liquid and gas occurs in the nozzle even when the spray cone does not meet each other inside the nozzle in the calculations.

As shown in Figure 4.5, when shallow recesses were applied, the spray angle was decreased and the spray became more stable, but the droplet size seemed slightly larger than no recess case. Comparing the non-impinging and the impinging cases, the thinner the lip thickness, the larger the spray angle and droplet size of the coaxial injector. This result is similar to the no recess case.

In addition, when a shallow recess was applied, droplets scattered outside the spray cone were less and the change of the spray angle was small. In addition, a mist-like flow of fine droplets was observed inside the hollow cone. In the average image shown in figure 4.7, it can be seen that the thinner the lip thickness is, the clearer the mist-like flow is. It is considered that as the lib thickness increases, the axial velocity of the liquid increases and the residence time in the recessed region decreases,

making the mist generation more difficult. Such mist is considered to be advantageous for facilitating ignition and achieving high combustion efficiency at the central region of the combustion chamber.
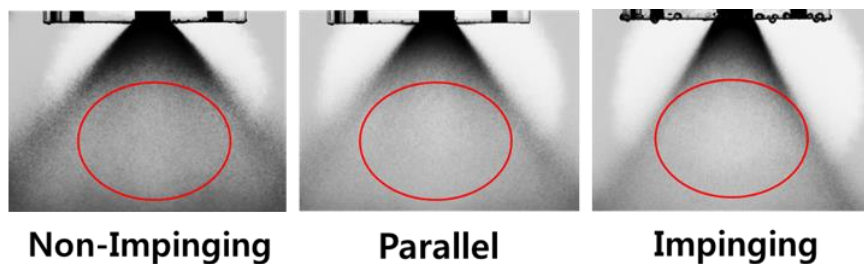
Figure 4.7 Averaged spray image in shallow recess case

4.3.3 Deep recess

Comparing the case of the shallow recess with that of the deep recess, in the deep recess case thick ligaments were observed and the boundary of spray became more apparent. This seems to be due to the fact that in the shallow recess case, the gas flow scratches and atomizes the liquid film at the outlet of the liquid injector, but in the case of deep recess, the momentum of the gas is reduced by the friction inside the recessed region. Commonly, in the deep recess case, the number of tiny droplets was smaller than that of the shallow recess case, so large droplets were dominant, and

mist was also difficult to observe. In addition, comparing the difference according to lip thickness, the number of tiny droplets was decreased when lip thickness was increased.

Chapter 5. CONCLUSION

The concept design of the 400N class methane rocket engine with single bipropellant injector was carried out to design the injector for the engine. The geometry of the combustion chamber and nozzle, cooling method, arrangement of the igniter, and type of injector were addressed. A gas centered swirl coaxial injector was adopted as a result of the numerical analysis of the combustion chamber designed on the basis of Kurpatenkov 's theory and four types of spray pattern.

The liquid injector was designed by modifying the theory of Kesaev and Dityakin, and the gas injector was designed by the Russian standard method and the theory of Vigor Yang. Coaxial injector design was also based on the theory of Vigor Yang.

The gas spray angle measured by the schlieren technique was about 80 degrees, which was 10 degrees different from the design value. The liquid spray angle was similar to the design value when the lip thickness was 3.0mm. In the case of 3.4mm, the liquid spray angle was similar to the spray angle of the gas injector, and when the lip thickness was 3.8mm, the shape of the spray was very uneven. The flow rate did not deviate significantly from the design value except when the lip thickness was 3.8 mm.

The spray characteristics of the coaxial injector according to the lip thickness and recess length were observed in 9 cases. In the case of no recess (RN = 0), the fluctuation of mass distribution and droplet size decreased as the lip thickness increased. In the case of shallow recess (RN = 1), a mist-like flow is observed inside the spray cone. In addition, the mist was more visible as the lip thickness decreased. In the case of deep recess (RN = 2), the atomization performance of the injector was lower than the case of shallow recess (RN=1).

Quantitative analysis such as accurate SMD measurement and measurement of mass flow distribution through patternator is required as the next step. In addition, based on the results of the cold test, it is necessary to study the optimization of the geometry of the combustion chamber and the injector to find a suitable injector for the engine. Finally, it must be verified through hot test.

References

[1] V. Ye. Alemasov, A. F. Dregalin, A. P. Tishin, *Theory of Rocket Engines* (in Russian), Moscow, Mashinostroene, 1989

[2] D. Kim, P. Han, J. Im, Y. Yoon, V. G. Bazarov, "Effect of Recess on the Spray Characteristics of Liquid–Liquid Swirl Coaxial Injectors", Journal of Propulsion and Power, Vol. 23, No. 6, 2007.

[3] 김선진, 이양석, 고영성, "친환경 추진제인 과산화수소와 액체메탄의 활용 역사와 연구 동향", 한국추진공학회지, Vol. 14, No. 4, 2010, pp. 46-58.

[4] "R-4D", Astronautix.com, http://www.astronautix.com/r/r-4d.html

[5] Northrop Grumman, "TR-308 Dual Mode Liquid Apogee Engine"

[6] 400N Bipropellant Apogee Motors, Orbital Propulsion Centre, http://www.space-propulsion.com/spacecraft-propulsion/apogee-motors/

[7] G. Schulte, "High Performance 400N MMH/NTO Bipropellant Engine for Apogee Boost Maneuvers", 35th AIAA/ASME/SAE/ASEE Joint Propulsion Conference & Exhibit, 20-24 June 1999, Los Angeles, CA, AIAA 99-2466

[8] NIIMASh, http://niimashspace.ru/files/2016/Raket_dvig_maloy_tyagi.pdf

[9] Yu. Z. Andreev, Ph.D Dissertation, Study of the dependences of the characteristics of 50 ... 400N NTO + UDMH thruster on the main parameters of a dual coaxial centrifugal injector and jet injectors for film cooling (in Russian),

NIIMASh, Nizhnyaya Salda, 2005

[10] http://novosti-kosmonavtiki.ru/forum/forum9/topic11175/?PAGEN_1=2, accessed July 28, 2018

[11] Rocket thruster 17D16, NIIMASh, http://www.niimashspace.ru/index.php /component/content/article/2-uncategorised/14-17d16

[12] W. M. Marshall, J. E. Kleinhenz, "HOT-FIRE TESTING OF 100 LB F LOX/LCH4 REACTION CONTROL ENGINE AT ALTITUDE CONDITIONS", NASA John H. Glenn Research Center, Cleveland, OH

[13] M. D. Klem, T. D. Smith, M. F. Wadel, M. L. Meyer, J. M. Free, H. A. Cikanek III, "LIQUID OXYGEN/LIQUID METHANE PROPULSION AND CRYOGENIC ADVANCED DEVELOPMENT", 62nd International Astronautical Congress, 2011, IAC-11-C4.1.5

[14] Yu. I. Ageenko, I. V. Pegin, "CONFIRMATION OF ENERGY EFFICIENCY IMPROVEMENT OF SMALL LIQUID ROCKET ENGINE WITH DEF"LECT-CENTRIFUGAL SCHEME MIXING SYSTEM (in Russian)", Journal of National Samara Aerospace University, Vol. 47, No. 5, Section 3, 2014

[15] A.A. Kozlov, A.G. Vorobiev, I.N. Borovik, "SMALL LIQUID ROCKET ENGINES (in Russian)", Moscow Aviation Institute, Moscow, 2013

[16] V. V. Bogdanov, R. Kh. Kutuev, "CALCULATIONAL-EXPERIMENTAL RESEARCH OF THE WORKING PROCESS OF THE SMALL ROCKET ENGINE ON THE ECOLOGICALLY PURE COMPONENTS OF GOx - C2H5OH (in Russian)", FGUP NIIMASh, Nizhnyaya Salda

[17] R. H. Kutuev, I. N. Lebedev, V. L. Salich, "DEVELOPMENT OF ADVANCED LOW THRUST ROCKET ENGINES WITH ECOLOGICALLY FRIENDLY PROPELLANTS (in Russian)" Journal of SSAU, Vol. 19, No. 3, 2009

[18] A.V. Kochanov, A. G. Klimenko, "Propects for the glow plug application of multiple starts of thrusters operating anergolic bipropellant (in Russian)", Journal of MGTU, Vol. Mechanical Engineering, No 2, 2015

[19] P. J. Robinson, E. M. Veith, A. A. Turpin, "Test Results for a Non-Toxic Dual Thrust Reaction Conttrol Engine", 41st AIAA/ASME/SAE/ASEE Joint Propulsion Conference & Exhibit, 10-13 July 2005, Tucson, Arizona, AIAA 2005-4457

[20] V. D. Kurpatenkov, Kh. V. Kesaev, "Calculation of Engine Combustion Chamber (in Russian)", Publishing house of MAI, Moscow, 1985

[21] G. P. Sutton, O. Biblarz, *ROCKET PROPULSION ELEMENTS*. 9th ed. WILEY

[22] A. P. Vasil'yev, V. M. Kudryavtsev et al., *FUNDAMENTALS OF THEORY AND CALCULATION OF LIQUID PROPELLANT ROCKET ENGINES* (in Russian). 2nd ed., Publishing House Vysshaya Shkola, Moscow, 1975

[23] Instability of processes in liquid rocket engines, HELPIKS.ORG, https://helpiks.org/4-76526.html

[24] M. I. Shtvelyuk, "Theoretical fundaments of liquid rocket engines design (in Russian)", Oborongiz, Moscow, 1960

[25] Yu. A. Bulygin, S. G. Valyukhov et al. "Parametric identification of hydrodynamics for channel of LRE (in Russian)", Publishing house VGTU,

Voronezh, Russia, 2001

[26] M. V. Dobrovolsky, *LIQUID ROCKET ENGNES: FUNDAMENTS OF DESIGN* (in Russian). 3rd ed., Publishing House of MGTU, Moscow, 2016

[27] N.V. Bezmenova, S.A. Shustov, FORMATION OF THE THERMAL AND GAS DYNAMIC CAE-MODELS OF VIRTUAL FLOWS OF COMBUSTION PRODUCTS IN CHAMBERS AND GAS GENERATORS OF LRE TAKING INTO ACCOUNT NON IDEAL FLOW OF THE WORKING PROCESSES: (In Russian), Publishing House of SSAU, Samara, Russia, 2010

[28] A. Ponomarenko, RPA: Tool for Rocket Propulsion Analysis Thermal Analysis of Thrust Chambers, July 2012 (v.3)

[29] 정기정, 이예승, 윤영빈,"450N 급 산소/메탄 엔진 연소실의 분석과 최적화", 제 55 회 KOSCO SYMPOSIUM 초록집 p. 87, 2017

[30] X. Wang, H. Huo, U. Unnikrishnan, V. Yang,"A systematic approach to high-fidelity modeling and efficient simulation of supercritical fluid mixing and combustion", Combustion and Flame, Vol. 195, pp. 203-215, 2018

[31] P. S. Leyevochkin, I. N. Borovik, Yu. S. Chudina, *Numerical simulation of conjugate heat transfer in the combustion chamber of a liquid-propellant rocket engine in the ANSYS CFX program,* Publishing House of MAI, Moscow, 2018

[32] R. Jeremy Kenny, Marlow D. Moser, James Hulka, Gregg Jones," Cold Flow Testing for Liquid Propellant Rocket Injector Scaling and Throttling", 42nd AIAA/ASME/SAE/ASEE Joint Propulsion Conference & Exhibit 9 - 12 July 2006, Sacramento, California, AIAA 2006-4705

[33] V. D. Kurpatenkov, Kh. V. Kesaev, *Calculation of Engine injectors* (in Russia), Publishing house of MAI, Moscow, 1987

[34] Losses in the LRE chamber, RocketEngines.ru, http://rocketengines.ru /rocket-engines-studying/base-of-knowledges/theory/losses-in-lpre- chamber.html

[35] A. A. Dorofeev, *Fundaments of Thermal Rocket Engines Theory: Theory, Calculation and Design* (in Russian), 2nd Ed, Publishing house of MGTU, Moscow, 2010

[36] V.D.Kurpatenkov, Kh. V. Kesaev, *Calculation of Engine Injector* (in Russian), Moscow, Publishing house MAI, 1987

[37] Yu.F.Dityakin, L.A.Klyachko et al., *Liquid atomization* (in Russian), 2nd Ed., Mashinnostroeine, Moscow, 1977

[38] V. Yang, M. Habiballah, J. Hulka, M. popp (Eds.), *Liquid Rocket Thrust Chambers: Aspect of Modeling, Analysis, and Design in Astronautics and Aeronautics*, Vol. 200, 2004

[39] L. Yang, M. Ge, M. Zhang, Q. Fu, G. Cai, "Spray Characteristics of a Recessed Gas-Liquid Coaxial Swirl Injector", Journal of Propulsion and Power, Vol. 24, No. 6, 2008

[40] A. Frrenberg, K. Hunt, J. Duesberg, "Atomization and mixing study", Rocketdyne Report No. RI/RD85-312, Canoga Park, California, 1985.

초   록

400N 급 소형 로켓 엔진은 정지궤도 위성의 원지점 엔진이나 유, 무인 우주선의 자세 제어용 등으로 널리 활용되고 있다. 기존 소형 로켓 엔진은 대부분 유독하고 부식성이 높은 자동점화성 추진제를 사용해 왔으나, 최근에는 재사용 발사체의 개발 및 유인우주탐사가 다시 시도되면서 미국, 러시아, 중국 등 우주 선진국에서 메탄을 연료로 하는 소형 엔진이 개발되고 있다.

메탄은 탄화수소이면서도 수소와 같이 극저온 액체에 속하며, 산소-메탄 추진제는 점화기가 필요한 비자동점화성이다. 따라서 그 특성은 현재 사용 중이거나 개발되었던 어떠한 소형 로켓 엔진용 추진제와도 다르다고 할 수 있다. 또한 메탄 엔진은 개발 역사가 짧고 실제 사용된 이력이 거의 없으므로 적합한 추진제의 혼합방식이나 분사기 형식이 정립되지 않은 것으로 보인다.

본 연구에서는 산소 / 메탄을 추진제로 하고 단일 이원 분사기를 가지는 소형 로켓 엔진의 연소실 및 분사 시스템의 기초 설계를 수행하였다. 연소실의 형상 설계 후 유한요소해석법을 통해 스월 및

제트 분사기의 조합에 따른 분무-혼합 시스템의 연소 패턴을 비교하였으며, 해석 결과에 따라 적합한 분사기의 유형을 기체 중심 이중 스월 분사기로 정하였다.

해당 형식의 분사기는 액체분사기 및 기체분사기의 개별적 성능과 형태를 계산한 후 산화제와 연료분사기를 동축에 배치하는 순서로 설계를 진행하였다. 수류 실험을 통해 기체 분사기의 립 두께와 리세스 길이의 변화에 따른 동축 분사기의 분무 특성을 확인하였으며, 리세스 길이가 없는 외부 혼합일 경우 립 두께가 증가할수록 액적의 크기가 감소하였고 시간에 따른 유량분포의 변동이 약화됨을 확인하였다. 리세스 길이가 임계 혼합에 해당할 경우 분무 원추 내부에 안개와 같이 미세한 액적으로 이뤄진 흐름이 관찰되었으며 이는 립 두께가 감소할수록 증가하였다. 리세스 길이가 내부 혼합에 해당할 경우 전체적으로 임계 혼합일 경우보다 분사기의 미립화 성능이 저하되었다.